



UNIVERSITY OF LEEDS

This is a repository copy of *Biomass explosion testing: Accounting for the post-test residue and implications on the results*.

White Rose Research Online URL for this paper:  
<http://eprints.whiterose.ac.uk/97354/>

Version: Accepted Version

---

**Article:**

Slatter, DJF, Sattar, H, Medina, CH et al. (3 more authors) (2015) Biomass explosion testing: Accounting for the post-test residue and implications on the results. *Journal of Loss Prevention in the Process Industries*, 36. pp. 318-325. ISSN 1873-3352

<https://doi.org/10.1016/j.jlp.2015.02.015>

---

© 2015, Elsevier. Licensed under the Creative Commons Attribution-NonCommercial-NoDerivatives 4.0 International  
<http://creativecommons.org/licenses/by-nc-nd/4.0/>

**Reuse**

Unless indicated otherwise, fulltext items are protected by copyright with all rights reserved. The copyright exception in section 29 of the Copyright, Designs and Patents Act 1988 allows the making of a single copy solely for the purpose of non-commercial research or private study within the limits of fair dealing. The publisher or other rights-holder may allow further reproduction and re-use of this version - refer to the White Rose Research Online record for this item. Where records identify the publisher as the copyright holder, users can verify any specific terms of use on the publisher's website.

**Takedown**

If you consider content in White Rose Research Online to be in breach of UK law, please notify us by emailing [eprints@whiterose.ac.uk](mailto:eprints@whiterose.ac.uk) including the URL of the record and the reason for the withdrawal request.



[eprints@whiterose.ac.uk](mailto:eprints@whiterose.ac.uk)  
<https://eprints.whiterose.ac.uk/>

# Biomass explosion testing: accounting for the post-test residue and implications on the results.

David J.F. Slatter, Hamed Sattar, Clara Huéscar Medina, Gordon E. Andrews, Herodotos N. Phylaktou & Bernard M. Gibbs.

*Energy Research Institute, University of Leeds, Leeds, UK.*

E-mail: [pm06djfs@leeds.ac.uk](mailto:pm06djfs@leeds.ac.uk)

## Abstract

This work uses the ISO 1 m<sup>3</sup> dust explosion equipment to study the explosion properties and combustion characteristics of pulverized biomass dust clouds. An unreported feature of this apparatus is that in rich concentrations only about half the dust injected is burned in the explosion, while the overpressures remain high. This work was undertaken to try to understand the mechanisms of these phenomena, through the accounting of the debris at the end of the explosion, some of which was found in the form of impacted “cake” against the vessel wall. One possible explanation is that the residue material was biomass dust blown ahead of the flame by the explosion induced wind, impacted on the walls where then the flame side underwent flame impingement pyrolysis and the metal (wall) side material was compacted but largely chemically unchanged. The results also show that the heat transfer insulation provided by the powder wall layer contributes to the higher observed pressures. The risk of explosion with significant overpressures remains at 100% in very rich environments (equivalence ratios of up to 6) although these environments are leaner than thought due to material sequestration within the “cake”. There was little indication that a rich combustion limit was approached, this was determined in standard testing equipment that has been modified and calibrated to handle larger quantities of powder than normal..

Keywords: *dust explosions, combustion residue, mass burnt*

## Nomenclature and abbreviations

Ø	equivalence ratio	P <sub>i</sub>	pressure at the moment of ignition
A/F	mass ratio of air to fuel	MEC	minimum explosible concentration
H/C	atomic ratio of hydrogen to carbon	TGA	thermogravimetric analysis
O/C	atomic ratio of oxygen to carbon	GCV	gross calorific value (mj/kg)
VM	volatile matter (wt. %)	SEM	scanning electron microscopy
FC	fixed carbon (wt %)	$\vec{q}$	local heat flux density (w/m <sup>2</sup> )
daf	dry, ash free basis	k	thermal conductivity (w/m k)
P <sub>max</sub>	maximum explosion pressure (bar)	∇T	temperature gradient(k/m)
K <sub>st</sub>	deflagration index (bar m s <sup>-1</sup> )	SMD	surface weighted mean diameter (microns)

## 1. Introduction

All published data for dusts and pulverized biomass show that the peak reactivity occurs between powder concentrations of 500 to 1500 g/m<sup>3</sup> Wilen et al. (1999). When this is converted into an equivalence ratio,  $\emptyset$ , based on the elemental composition formula of the powder, then most of these peak reactivity mixtures fall between  $\emptyset$  of 3 to 5, as shown in Table 1.

Table 1: Most reactive concentrations for different fuels.

Material	Chemical Formula CH <sub>x</sub> O <sub>z</sub>	$\emptyset=1$ g/m <sup>3</sup> - daf	Concentration	$\emptyset$ for	Pmax	Equipment Used	References
			(g/m <sup>3</sup> ) for Pmax -daf	Pmax -daf	Pmax		
			Concentration	$\emptyset$ for	Kst		
			(g/m <sup>3</sup> ) for Kst- daf	Kst - daf	Kst		
Cellulose (22 $\mu$ m)	(C <sub>6</sub> H <sub>1.67</sub> O <sub>5</sub> ) <sub>n</sub>	235	500	2.13	9.4	1m <sup>3</sup> vessel	(Bartknecht, 1989)
			500	2.13	204		
Lycopodium	CH <sub>1.58</sub> O <sub>0.71</sub>	118	427	3.62	5.5	20L sphere	(Amyotte et al., 1990)
			427	3.62	46		
Corn Flour	CH <sub>2.01</sub> O <sub>0.80</sub> (This study)	212	339	1.60	6.0	10.3m <sup>3</sup> vessel	(Kumar et al., 1992)
			339	1.60	155		
Corn Flour	CH <sub>2.01</sub> O <sub>0.80</sub> (This study)	212	635	2.99	9.0	20L sphere	(Skjold et al.,2005)
			635	2.99	160		
Corn Flour	CH <sub>2.01</sub> O <sub>0.80</sub> (This study)	212	635	2.99	8.4	20L sphere	(Tamanini and Ural, 1992)
			635	2.99	158		
Forest Residue (275 $\mu$ m)	CH <sub>1.58</sub> O <sub>0.71</sub>	210	683	3.25	10.8	1m <sup>3</sup> vessel	(Garcia Torrent et al., 1998)
			1367	6.51	267		
Cork Dust (71.4 $\mu$ m)	CH <sub>1.62</sub> O <sub>0.70</sub>	204	378	1.86	7.5	22.7L vessel	(Pilão et al, 2004)
			426	2.09	60		
Cork Dust (212 $\mu$ m)	CH <sub>1.62</sub> O <sub>0.70</sub>	204	426	2.09	6.0	22.7L vessel	(Pilão et al, 2004)
			473	2.32	23		
Polyethylene	(C <sub>2</sub> H <sub>4</sub> ) <sub>n</sub>	81	500	6.17	6.47	20L sphere	(Cashdollar, 1996)
			500	6.17	59		
Bituminous Coal	CH <sub>0.84</sub> O <sub>0.66</sub>	102	253	2.48	7.7	1m <sup>3</sup> vessel	(Wiemann, 1987)
			368	3.61	95		
Graphite (4 $\mu$ m)	C	104	250	2.40	6.6	20L sphere	(Denkevits and Dorofeev, 2005)
			25	2.40	70		
Graphite (25- 32 $\mu$ m)	C	104	200	1.92	5.9	20L sphere	Denkevits and Dorofeev, 2005)
			250	2.40	24		
Graphite (40- 45 $\mu$ m)	C	104	250	2.40	6.1	20L sphere	Denkevits and Dorofeev, 2005)
			500	4.81	21		
Methane	CH <sub>4</sub>	70	74	1.06	7.1	5L vessel	(NFPA68, 2007)
			74	1.06	55		
Propane	C <sub>3</sub> H <sub>8</sub>	77	86	1.13	7.9	5L vessel	(NFPA68, 2007)
			86	1.13	100		
Ethylene	C <sub>2</sub> H <sub>4</sub>	81	106	1.30	8.0	5L vessel	(NFPA68, 2007)
			106	1.30	243		
Hydrogen	H <sub>2</sub>	34	55	1.60	6.8	5L vessel	(NFPA68, 2007)
			55	1.60	550		

This is true for most other dusts, also shown in Table 1. The Table also illustrates the strong difference between dusts and gases over the equivalence ratio at which the peak reactivity occurs. This work was undertaken to investigate why this occurs. This is most relevant to pulverized biomass and coal as the mills operate with air transport of the dusts to the burners

using rich mixtures that are assumed not to be flammable. The experimental results from this work (and that of others) indicate instead that these mixtures are very flammable.

One of the issues that we highlight in this work is that a large proportion of the mass of dust injected into the standard 1 m<sup>3</sup> ISO vessel was found as residue in the vessel after the test. This residue consisted of light and dark particles suggesting that it was not a homogeneous mixture; possibly made up of both burnt and unburnt material.

In dust explosions it is also known that the maximum pressure does not fall significantly as more dust is added. This suggests that the additional fuel may not be acting as a heat sink, as would be expected if it is in the dust cloud but not burned. It was considered that one explanation was that the expanding flame in the centre of the vessel generates a wind ahead of the flame that would entrain the outer dust particles and move them onto the wall ahead of the flame. This would then form a layer on the internal surface of the vessel. Thus the concentration of the mixture that the flame propagated through would be much lower than the injected mixture concentration. Depending on the thickness of the layer this could result in the outside of the compressed particle layer being scorched by the advancing flame front while the particles closer to the wall would be less burned. Also this wall layer of dust would act as insulation which would reduce the rate of cooling after the explosion and this possibility was investigated in the present work.

## 2. Experimental Techniques

### 2.1 Materials

Cornflour and Kellingley Coal were used as reference materials. The biomass dust used was pine wood dust supplied in pulverised form by Drax power station. Residues from the standard 1m<sup>3</sup> ISO dust explosion vessel for the most reactive concentrations (higher  $K_{st}$ ) were also sampled and analysed in a follow up paper. The elemental, proximate and size analysis are included for the samples tested, in Tables 2 and 3.

Table 2: elemental, proximate and stoichiometry of the fuels.

ELEMENTAL ANALYSIS (% by mass)					
	<b>C</b>	<b>H</b>	<b>N</b>	<b>S</b>	<b>O</b>
<b>Corn flour</b>	37.8	6.3	0.1	0.0	40.4
<b>Drax biomass dust</b>	43.9	6.2	0.6	0.0	37.6
<b>Coal</b>	51.6	4.4	2.0	2.0	15.0
PROXIMATE ANALYSIS (% by mass)					
	VM	FC	Ash	Moisture	
<b>Corn flour</b>	77.8	6.8	3.8	11.6	
<b>Drax biomass dust</b>	79.5	8.7	8.2	3.5	
<b>Coal</b>	33.2	41.8	22.6	2.4	
STOICHIOMETRY					
	A/F (daf)	g/m <sup>3</sup> (daf)	g/m <sup>3</sup> (as received)		
<b>Drax biomass dust</b>	5.7	212.3	251.0		
<b>Coal</b>	6.3	189.2	214.2		
<b>Corn flour</b>	9.6	125.3	167.0		

Table 3: Size distribution for different fuels based on surface weighted mean diameter (SMD).

	Drax biomass dust	coal	cornflour
D [3, 2] - SMD	26.1	12	7.4
d (0.1)	18.7	5	7.9
d (0.5)	64.4	25.5	14.1
d (0.9)	196.2	65.3	21.7

Each d value is the diameter of the particle size at the corresponding sample volume. So a d (0.1) of 18.7 is the diameter (18.7 microns) at which 10% (by volume) of the sample has been reached. An important observation to make from this is that the d (0.1) of Drax Biomass is only slightly smaller than the d (0.9) of cornflour.

## 2.2 Dust explosions

Dust-air mixtures were exploded in a 1.138 m<sup>3</sup> closed cylindrical steel vessel, with a length to diameter ratio of unity Sattar et al., (2012). The vessel was constructed to the specifications of the ISO 6184/1 (1985) standard for the determination of explosion indices of dusts. Two types of dust injectors were used in the ISO 1 m<sup>3</sup> explosions, the standard 1 m<sup>3</sup> C-ring and a new disperser developed by the authors for biomass injection. This spherical injector replaced the C ring and was a simple spherical ball 110mm diameter with an array of grid plate type holes in the outer hemisphere. The spherical injector was used as fibrous biomass could not pass through the C-ring. Coal dust was placed in a 4.5 liter external chamber, connected to the perforated C-ring inside the vessel via a fast acting pneumatic ball valve. The “dust pot” was pressurised with air to 20 bar (g). For biomass an additional 5L extension was added to the dust pot to accommodate biomass of low bulk density Sattar et al. (2012a,b). The main vessel pressure was reduced to 933 mbar(a) using a vacuum pump. The release of the pressurised contents of the dust pot into the main vessel resulted in an increase in vessel pressure by 80 mbar, giving a total nominal pressure prior to ignition of 1013 mbar(a) (1 atm). The ignition delay was set to the standard value of 0.6s with the standard 5L dust holder and C-ring injector system, whereas the ignition delay when the system was set up for biomass (10L dust holder and spherical injector) was found to give the same turbulence levels at 0.5s ignition delay. The inlet air valve was closed just prior to ignition. Ignition was effected by two 5kJ Sobbe igniters firing into a small perforated hemispherical cup in the center of the vessel (in order to limit the problems of directional ignition effects, as shown to be necessary by Phylaktou *et al.* (2010). Explosion pressure histories were monitored using a piezoresistive pressure transducer mounted in the wall of the vessel. The rate of pressure rise was calculated by differentiation of a section of the pressure signal after elimination of electronic noise, by a degree of smoothing.

## 2.3 Rate of pressure loss

The rate of pressure loss was calculated on the basis of the time taken for 10% reduction of pressure from the peak pressure achieved during the test (see Fig. 8) - 10% was chosen as it was deemed short enough to show differences in the pressure decay rate under the different test conditions.

## 2.4 Flame temperatures

The theoretical adiabatic flame temperatures at constant pressure, were calculated using in-house FLAME software. This software calculates equilibrium flame composition and adiabatic temperatures for a range of fuels and combustion conditions using the C, H, N, S, O, ash, and moisture compositions as well as the GCV obtained as mentioned in section 2.2.

## 2.5 Other equipment

The elemental composition of all materials was measured using a Flash 2000 Thermo Scientific Analyzer with single reactor for the determination of CHNS elements only whereas the percentage of oxygen was found by difference.

Moisture, volatile matter and fixed carbon contents were measured using a Shimadzu TGA-50 thermo gravimetric analyser. The ash content was calculated by subtraction.

The atomic ratios to carbon of hydrogen (H/C) and oxygen (O/C) were used to calculate the air to fuel ratios (A/F) and the stoichiometric fuel to air ratio of all samples as explained in Huescar Medina et al. (2013).

The particle size analysis was done on a Malvern Mastersizer 2000, using the laser diffraction technique by assuming the shape of the particle as spherical. The sample is mixed with water into a paste and then added to a water pump that flows the particles through the analyser's cell suspended in the water. The particles in a cell are passed through a focused laser beam which scatters the light at an angle that is inversely proportional to the size of a particle. This angular intensity of the scattered light is measured by a series of photosensitive detectors. The map of scattering intensity versus angle is used to calculate the particle size. To ensure that this is accurate the refractive index of each material must be matched with that of a similar material within the database. However as fibrous biomass particles are not spherical, and this instrument measures the light diffracted from the actual particle and then gives it the size of a spherical particle that would diffract that light. This is not the spherical particle of the same mass, volume or surface area as the actual particle. Nevertheless, the method does enable the size distribution of materials to be compared roughly.

Each result of particle size distribution is an average of 10 measurements, where there was no fall out or clumping of the particles in suspension.

## 3. Results

### 3.1 Burned mass as a proportion of the injected mass

A key feature of explosions in the ISO 1 m<sup>3</sup> vessel is that a large fraction of the mass of dust injected does not burn and is left as a residue in the vessel at the end of the explosion. The burned concentration was the mass of dust injected (which was the mass placed in the external pot minus the mass of dust remaining in the pot after the explosion, about 5-10%) minus the mass of dust collected from the test vessel at the end of the explosion. Full details of these procedures are given by Sattar et al. (2012a,b). Most of the literature on dust explosions does not mention that a large fraction of the dust injected into the ISO 1 m<sup>3</sup> vessel does not burn (nor do they report the mass fraction remaining in the holding pot) and hence the concentrations reported are not the dust concentrations that the flame propagates through but a nominal "intended" concentration. Pilao et al. (2004), in a wide ranging work on cork dust explosion hazards also detailed the large proportion of the cork dust that was left as debris at the end of the explosion.

For some dusts, such as milk powder, the residue was left adhered to the vessel walls. Photographs of the wall "cake" from milk powder explosions are shown in Figs. 1 and 2. They clearly show that the side against the metal wall was not burned or pyrolysed, but the side exposed to the flame was pyrolysed by the flame. Very few dusts we have tested had formed a cake residue and in all other dust explosions presented here, the residue was left as a powder on the bottom of the ISO 1 m<sup>3</sup> dust explosion vessel.

In the ISO 1 m<sup>3</sup> explosion tests, two types of dust injectors were used (as described earlier), the standard C-ring and the spherical disperser. In the graphs that follow, the results are labeled to indicate the type of dust followed by “C-ring” or “spherical”, to identify which dust disperser was used. Both dispersers have previously been tested and calibrated and the procedure is the same as that given in Sattar (2013) for the 10L pot.



Figure 1: Milk powder “cake”, wall-touching side



Figure 2: Milk powder “cake” flame-touching side

This work presents the results for cornflour dust, pine wood biomass from Drax power station, and comparison is made with pulverized Kellingley coal and, where relevant, with turbulent methane explosions. This analysis was used to determine the stoichiometric concentration on a dry ash free basis (daf) and on this basis the concentration that was injected or burned in the explosion was expressed as an equivalence ratio; effectively assuming the direct oxidation of the species identified by the chemical formulae of the powders.

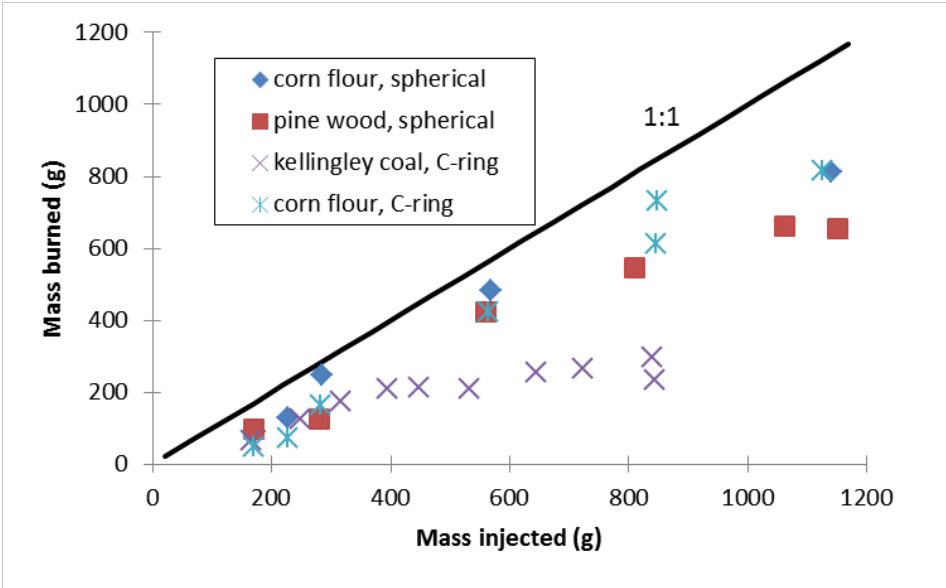


Figure 3: Mass of powder burned as a function of mass injected

Figure 3 shows that the mass of material burned had a non-linear relationship with the mass injected and that coal behaved differently than biomass. In Fig.4 the unburned mass fraction is

also expressed in terms of the injected equivalence ratio and the actual burned equivalence ratio.

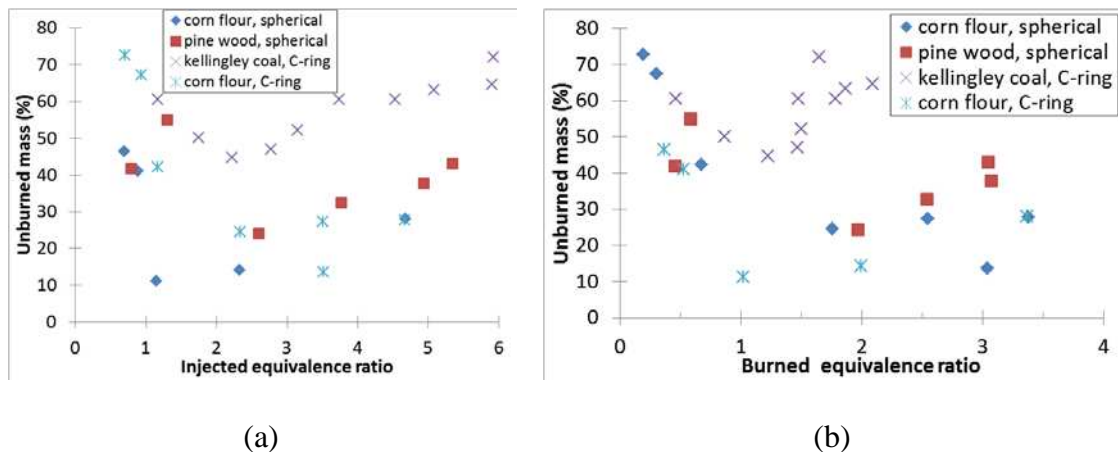


Figure 4: Fraction of mass burned as a function of (a) injected and (b) burned equivalence ratio

For coal and biomass up to an injected quantity of  $400 \text{ g/m}^3$  50% of the injected dust did not burn. This is roughly the condition for burning with sufficient air to oxidise the fuel that was burned. However, for larger injected quantities an increasing fraction of powder did not burn and this is the area of richer than stoichiometric combustion. For coal there was a very sharp increase in the unburned proportion after  $400 \text{ g}$  injected, as at  $600 \text{ g}$  only  $250 \text{ g}$  burned and at  $800 \text{ g}$  injected this was increased to  $300 \text{ g}$  that burned. Thus, 63% was not burning for high injected concentrations. For biomass at  $1000 \text{ g/m}^3$  injected  $700 \text{ g/m}^3$  was burned and this is only 30% not burning. Figure 3 shows that there was considerable data scatter around the above numbers, but it is clear that for rich burning mixtures coal and biomass behaved quite differently in terms of the proportion of the injected dust that burned. As shown in Fig. 4 when the data is changed from mass to an equivalence ratio (based on either the injected or burned fuel) the different behaviour of coal to biomass remains clearly evident.

This is important in pulverising mills and pneumatic conveyor systems as dust concentrations are maintained in the rich zone by design in the anticipation that combustion, if initiated, will be weak. In the present results the directly comparable concentration to the industrial applications is the injected powder concentration or equivalence ratio. In the first instance the present results clearly show that biomass will burn more readily at a much higher fraction than coal. In the next section we will show that the highest overpressures and reactivity rates were also encountered in the rich mixtures.

### 3.2 $K_{st}$ and $P_{max}$ for biomass and coal dusts

The maximum pressure and the  $K_{st}$  reactivity parameter results are shown as a function of the injected burnt equivalence ratio in Figs. 5 and 6. Cornflour dust was tested on the C ring standard injector and on the new design for biomass, the spherical injector, which had been calibrated on propane to achieve the same turbulence level as for the C injector. The results in Figs. 5 and 6 show that there was good agreement in  $P_{max}$  at 9 bar and good agreement in the  $K_{st}$  of 120 bar m/s for the same burned equivalence ratio. Figures 5 and 6 show that Kellingley coal and pine wood dust had very similar peak pressures and  $K_{st}$  values, which were significantly lower than that for cornflour.

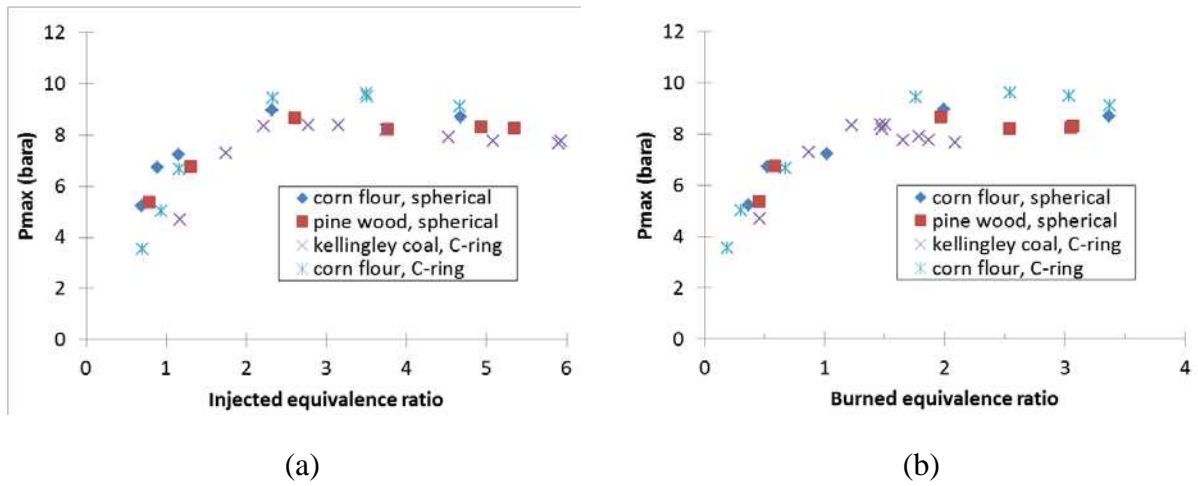


Figure 5: Maximum pressure as a function of the (a) injected and (b) burned equivalence ratio

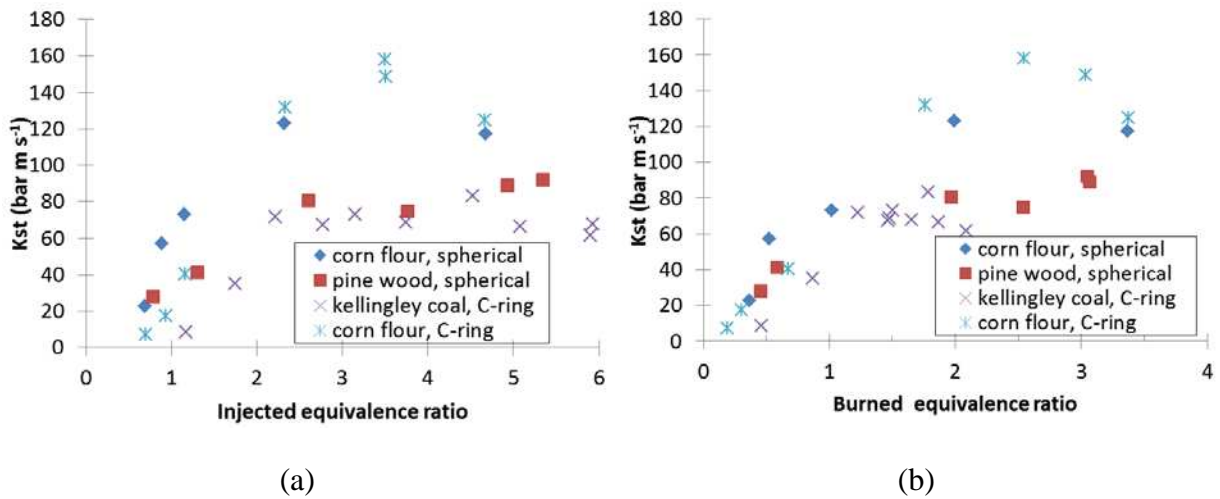


Figure 6:  $K_{st}$  as a function of the (a) injected and (b) burned equivalence ratio.

A significant feature of Figs. 5 and 6, for both coal and biomass is that although the reactivity and  $P_{max}$  increases with burned mass  $\phi$  in the lean region and continues to increase in the rich region with the peak reactivity and  $P_{max}$  occurring for  $\phi$  of 2 or richer. There was no significant decrease in  $K_{st}$  or  $P_{max}$  up to burned  $\phi$  of 3-4. In terms of injected  $\phi$  (which is more practically relevant parameter) it is evident that combustion still takes place and that strong and significant pressures are generated for both coal and biomass for equivalence ratios of 6 and beyond, with the reactivity of biomass being higher than coal for the two types of biomass investigated. This clearly shows that the risk of explosion with significant overpressures remains at 100% in very rich environments with little indication that a rich combustion limit is “near” and this was determined in standard testing equipment that had been modified and calibrated to handle larger quantities of powder than normal. This challenges the general industry assumption that operating in very rich conditions is safe and demonstrates that if there is indeed a rich limit for dusts the present standard testing equipment are not capable of measuring it.

This behaviour of rich dust/air mixtures is different to that of gas/air mixtures, which have a rich limit at much lower equivalence ratios than tested in this work. Some potential reasons for this are:

- As shown by adiabatic flame temperature calculations, rich mixtures continue to have high flame temperatures over a wide range of rich  $\phi$ .
- In a closed vessel explosion there is a fixed mass of air and the dust is injected into this and does not displace any air. There is a fixed heat release of 3MJ per kg of air (Drysdale, 1992) irrespective of the fuel. For gases, rich mixtures have higher volume concentration and more air is displaced as the gas concentration is increased. So in a fixed volume system for rich dust/air mixtures the energy available to be released is greater than the equivalent rich gas/air mixture because of the relative mass of available air (which is the controlling reactant in rich mixtures).
- Another possible contribution to these phenomena is that although the initial mixture pressure is 1 atm, before the powder can burn it has to turn into pyrolysis gases and when these gases are added to the fixed system volume the initial mixture pressure effectively goes up. So as the hot flame kernel develops from the ignition point progressively more volatiles are driven off the dust cloud ahead of the flame and this would have the effect that each combustion step would take place in comparatively higher pressures than the equivalent gas/air mixture. This will have a compounding effect on the final explosion pressure  $P_{max}$  for dusts resulting in higher overpressures than equivalent gas air mixtures. This effect could be partially or totally counter-balanced by the excess dust particles acting as a heat sink.
- It is more difficult to explain why the mixture reactivity,  $K_{st}$ , is so high for rich mixtures and why the maximum reactivity is not close to  $\phi = 1$  as it is for gases. Part of the reason is that reactivity is related to flame temperature, but this comes back to the reason why the flame temperature does not peak until about  $\phi = 2$ . Another possible explanation is that the definition of the equivalence ratio for dusts is based on the chemical composition of the solid particle rather than the actual combustion chemistry which is defined by the composition of the pyrolysis gases (which is not known).

Figure 3 shows that roughly 50% of the injected mass of dust did not participate in the explosions. It was argued by Sattar et al (2012 a,b) that if the peak pressure was close to that expected for adiabatic explosions, as shown in Fig. 5, then the dust that does not burn cannot be in suspension when the flame passes over it as it would then cool the flame and prevent the peak adiabatic pressure and peak reactivity from being achieved. It could be argued that this is what in fact does happen for near stoichiometric mixtures, that is why the expected peak pressure is low and the reactivity is lower than expected.

It could also be expected that if there were dust particles that did not burn then these would be the larger particles and it would then be expected that the debris would have a larger size distribution than the original biomass. However, Sattar et al. (2012a, b) showed that this was not the case for biomass dusts, showing the same size distribution for the original material and the debris.

Further to the effect of increasing system pressure due to the progressive release of more volatiles as the flame grows and the potential counter-balancing effect of the heat sink (argued above); there is evidence from the present work that the unburned dust ahead of the flame is compressed against the wall. In a constant volume explosion 90% of the fuel burns in the last 10% of flame travel and this results in dust being compressed against the wall and even in the

cases where it does not stick on the wall it temporarily forms an insulative layer having an effect on the heat loss from the system. As the explosion wind subsides the loose powder particles fall to the vessel floor.

Evidence that this deposit layer forms is presented below in terms of it acting as an insulating layer that reduces the rate of cooling of the vessel and hence changing the rate of pressure loss after the peak pressure has occurred.

### *3.3 Pressure decay in the ISO 1m<sup>3</sup> explosion vessel: comparison of gas and dust explosions*

The rate of pressure decay from the 1m<sup>3</sup> vessel following the explosions was recorded as shown in Fig. 7. The pressure decay was due to heat loss; not leakage, as the vessel is hermetically sealed. The decay rate was measured for the period immediately after the peak explosion pressure, until the pressure was reduced to 90% of its peak value, as shown in Fig. 8. A faster decay indicated greater heat losses and Fig. 8 shows that for a gas explosion the heat loss was much faster than for a dust explosion for similar peak pressure and hence similar peak temperatures. It is considered that the rate of pressure loss is related to the thickness of dust layer that is formed transiently on the wall at the end of the explosion. The dust acts as an insulating layer at the moment the flame hits the wall. The rate of pressure loss should then be a function of the thickness of the dust on the wall.

The residue recovered from the vessel was subtracted from the mass loaded into the dust pot (minus any dust left in pot) to give the “mass burnt” value (the mass injected is the weighed mass into the external pot minus the mass left in the pot). The measured rate of pressure loss is plotted as a function of the calculated compressed dust wall layer assuming uniform thickness, in Fig. 8. There are two trends in the pressure loss rate: firstly, there is a maximum pressure loss rate which corresponds with the peak flame temperature; secondly, the thickness increases as more dust is used in the explosion and the mass of unburned dust increases. This increased thickness reduces the rate of pressure loss even though for rich mixtures the peak pressure and therefore temperature remain high.

The differences in the rate of pressure decay and hence heat loss with the different powders probably reflects their different capability to form a stable layer when compressed and also to differences in the thermal conductivity of the different species.

The pressure decay rate was a function of the peak temperature of the dust explosion flame and thus peak adiabatic flame temperature predictions are required to understand the pressure loss rate data.

The temperature difference between the flame and the wall would drive the convective heat transfer and any dust layer would act as an insulating layer which would reduce the rate of heat loss to the metal walls. The flame temperatures were calculated using in house FLAME software, for the equivalence ratio,  $\phi$ , based on the mass burned (injected mass – residual mass). The flame temperatures were computed at constant pressure and are not strictly valid for the constant volume conditions of the closed vessel explosion. However, the two temperatures are related and this work was concerned with understanding the trends in the explosions. The differential form of Fourier's Law of thermal conduction shows that the local heat flux density,  $\vec{q}$ , is equal to the product of thermal conductivity,  $k$ , and the negative local temperature gradient,  $-\nabla T$ . The heat flux density is the amount of energy that flows through a unit area per unit time.

$$\vec{q} = -k\nabla T \quad (1)$$

Therefore if the temperature difference is constant it is only the thermal conductivity of the gas/vessel boundary that dictates the rate of pressure loss. Also changes in the peak flame temperature due to the dust composition will influence the pressure decay.

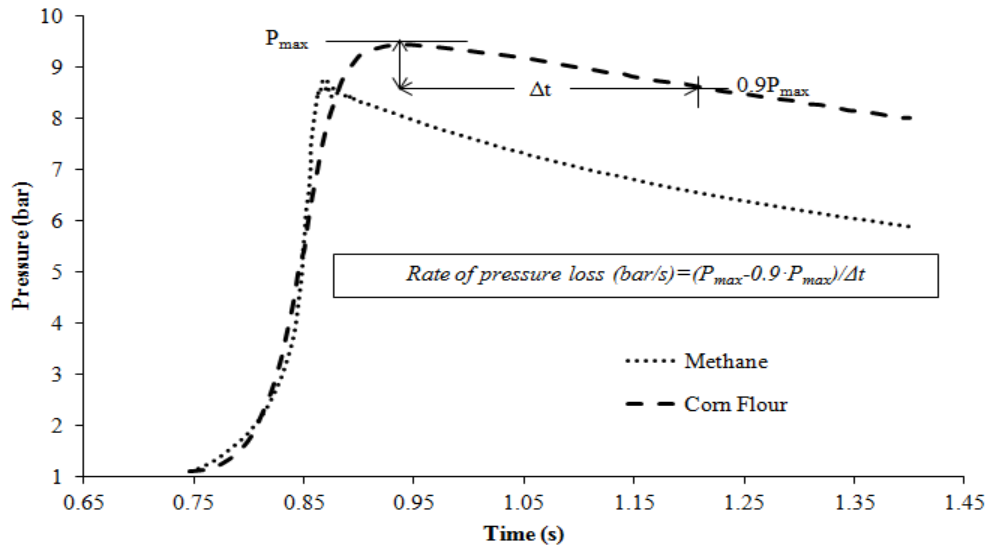


Figure 7: Rate of pressure loss for methane and corn flour

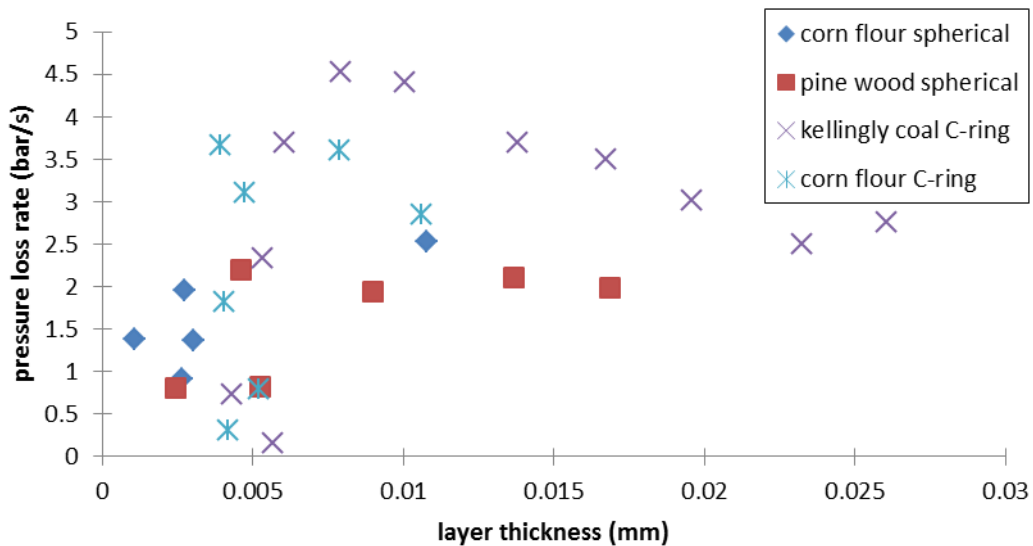


Figure 8: Pressure loss rate, after the peak pressure as a function of the calculated dust wall layer thickness.

Figure 9 shows the rate of pressure decay after the peak pressure in the explosion as a function of the flame temperature. This shows as expected the fastest decay for methane-air explosions with no deposits on the wall. Comparison with coal and cornflour at the same temperature gave over 50% lower pressure decay rate, indicating the presence of an insulating deposit. The peak pressure decay rate for dusts was 30% lower than for methane. This shows

that the deposit thicknesses (up to 0.02 mm) in Fig. 8, were sufficient to reduce the heat losses.

Figure 10 shows the rate of pressure decay as a function of the burned dust equivalence ratio. This shows unexpected results when compared with Fig. 9. The peak pressure decay does not occur at the peak flame temperature. FLAME predicts that the peak temperature should occur just richer than  $\phi=1$ , as for gases. It is not known why in dust explosions the highest pressure and the peak reactivity occur for rich mixtures, but this is a feature of HCO composition dust explosion generally and is not specific to biomass. Thus the reason the peak pressure decay occurs for rich mixtures in Fig. 10 is that experimentally this is where the peak temperature occurs, which gives the peak pressure. At this mixture FLAME predicts a low temperature, as would occur for a gas mixture, which accounts for the peak in the rate of pressure loss in Fig. 9 at 1500K, which is the predicted adiabatic temperature for  $\phi \sim 2$ .

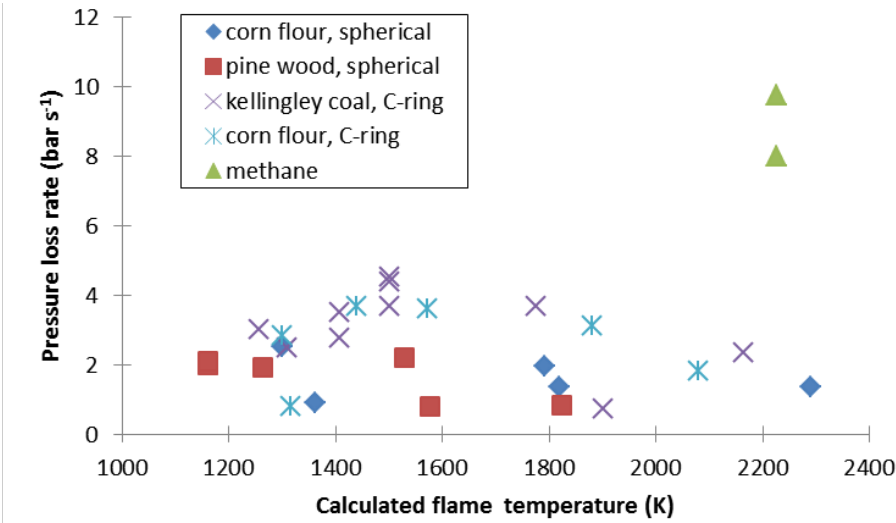


Figure 9: Rate of pressure decay as a function of the adiabatic flame temperature at constant pressure

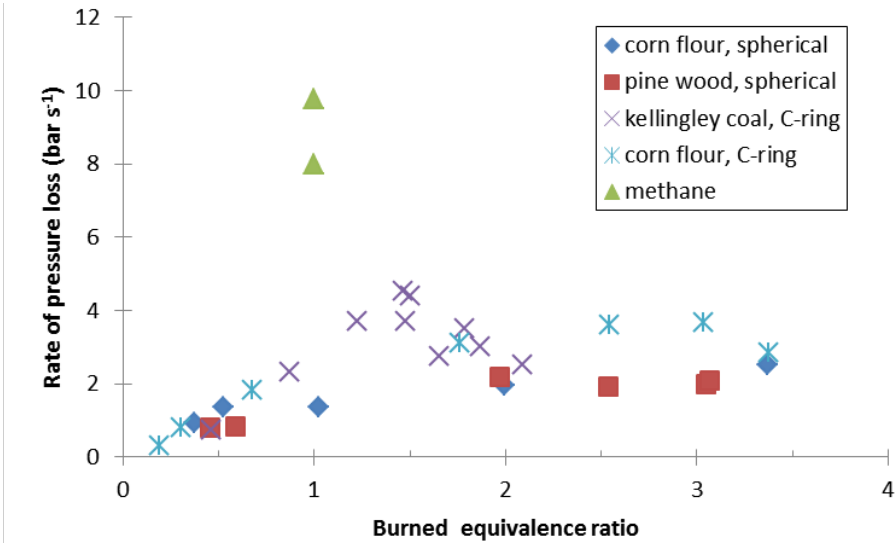


Figure 10: Rate of pressure loss as a function of the burned dust  $\phi$

#### 4. Conclusions

A key feature of explosions in the ISO 1 m<sup>3</sup> vessel is that a large fraction of the mass of dust injected does not burn and is left as a residue in the bottom of the vessel at the end of the explosion. Most of the literature on dust explosions does not mention that a large fraction of the dust injected into the ISO 1 m<sup>3</sup> vessel does not burn and hence the concentrations recorded are not the dust concentrations that the flame propagates through.

The results support the model of dust explosions where the expanding flame generates a wind ahead of the flame that entrains dust ahead of it and reduces the concentration of dust that the flame burns into. As the flame approaches the wall and the pressure rises, this wind is reduced to zero and the inertia in the particles carries them to the wall, where the pressure rise compresses them. At no stage do these particles participate in the heat release of the explosion. As the flame impinges on the wall with the residue layer the outer surface is heated and undergoes pyrolysis. It should be noted that if there is no significant heat release from these deposits then it is expected that overall the deposits left as a dust after the explosion will not be greatly different from the raw biomass dust, as shown by Sattar (2012a, b). The deposits on the wall act as thermal insulation and this reduces the rate of heat loss and hence the rate of pressure decay from the explosion vessel after the peak pressure. This pressure decay was shown to be slower with biomass dust explosions than for gaseous explosions where no insulative layer is formed.

The results also show that the risk of explosion with significant overpressures remains at 100% in very rich environments with little indication that a rich combustion limit is “near” and this was determined in standard testing equipment that have been modified and calibrated to handle larger quantities of powder than normal. This challenges the general industry assumption that operating in very rich conditions (for example in mills and pneumatic conveying ducts) is safe and demonstrates that if there is indeed a rich limit for dusts, the present standard testing equipment are not capable of measuring it.

#### Acknowledgements

The authors gratefully acknowledge the financial contribution from John and Dorothy Slatter. We would like to thank Drax Power for the donation of power station pulverised pine dust.

#### References

- Amyotte, P. R., Baxter, B. K. & Pegg, M. J. (1990) Influence of initial pressure on spark-ignited dust explosions. *Journal of Loss Prevention in the Process Industries*, 3, 261-263.
- Bartknecht, W. (1989) *Dust explosions: Course, Prevention, Protection*, Berlin Springer.
- Cashdollar, K. L. (1996) Coal dust explosibility. *Journal of Loss Prevention in the Process Industries*, 9, 65-76.
- Denkevits, A. & Dorofeev, S. (2005) Dust explosion hazard in ITER: Explosion indices of fine graphite and tungsten dusts and their mixtures. *Fusion Engineering and Design*, 75-79, 1135-1139.
- Drysdale, D. (1992) *An Introduction to Fire Dynamics*, Wiley-Interscience, New York.
- Garcia-Torrent, J., Conde-Lazaro, E., Wilén C., Rautalin A. (1998) Biomass dust explosibility at elevated initial pressures. *Fuel*, 77, 1093-1097.

- Huéscar Medina, C., Phylaktou, H.N., Sattar, H., Andrews, G.E., Gibbs, B.M. (2013) The development of an experimental method for the determination of the minimum explosible concentration of biomass powders, *Biomass and Bioenergy*, 53, 95 -104.
- Kruger, R.A., Fly ash beneficiation in South Africa: creating new opportunities in the market-place. Ash Resources, PO Box 3017, Randburg 2125, South Africa
- Kumar, R. K., Bowles, E. M., Mintz K.J. (1992) Large-scale dust explosion experiments to determine the effects of scaling on explosion parameters. *Combustion and Flame*, 89, 320-332.
- NFPA68 (2007) *Standard on explosion protection by deflagration venting*, National Fire Protection Association, Batterymarch Park, Quincy, MA 02269.
- Pilao, R., Ramalho, E. & Pinho, C. (2004.) Influence of initial pressure on the explosibility of cork dust/air mixtures. *Journal of Loss Prevention in the Process Industries*, 17, 87-96.
- Slatter, D., Sattar H., Andrews, G.E., Gibbs, B.M., Phylaktou H.N. (2014) **Biomass explosion residue analysis**. *Journal of Loss Prevention in the Process Industries*. Submitted.
- Sattar, H., Andrews, G.E., Gibbs, B.M., Phylaktou H.N. (2013) *calibration of a 10L volume dust holding pot for the 1m<sup>3</sup> standard vessel for use in low bulk density biomass explosibility testing*, 2013, 7th international seminar on fire and explosion hazards.
- Sattar ,H;Slatter, D; Andrews G.E; Gibbs B.M; Phylaktou H.N. (2012a.) Pulverised Biomass Explosions: Investigation of the Ultra Rich Mixtures that give Peak Reactivity. Proc. of the IX International Seminar on Hazardous Process Materials and Industrial Explosions (IX ISHPMIE), Krakov, 2012a.
- Sattar, H., Phylaktou, H.N., Andrews G.E. and Gibbs, B.M. (2012b.) Explosions and Flame Propagation in Nut-shell Biomass Powders. Proc. of the IX International Seminar on Hazardous Process Materials and Industrial Explosions (IX ISHPMIE), Krakow.
- Skjold, T., Arntzen, B. J., Hansen O. R., Taraldset O. J., Storvik I. E. and Eckhoff R. K. (2005). Simulating Dust Explosions with the First Version of DESC. *Process Safety and Environmental Protection*, 83, 151-160.
- Tamanini, F. & Ural, E. A. (1992) FMRC studies of parameters affecting the propagation of dust explosions. *Powder Technology*, 71, 135-151.
- Wiemann, W. (1987) Influence of Temperature and Pressure on the Explosion Characteristics of Dust/Air and Dust/Air/Inert Gas Mixtures. In: Cashdollar, K. L. & Hertzberg, M. (eds.) *Industrial Dust Explosions, ASTM STP 958*. Philadelphia: American Society for Testing and Materials.
- Wilén, C., Moilanen, A., Rautalin A., Torrent J., Conde E., Lödel R., Carlson D., Timmers P. & Brehm K. (1999) Safe handling of renewable fuels and fuel mixtures. *VTT Publications, Finland*, 394, 1-117.